Drivers of the Northern Extratropical Eddy-Driven Jet Change in CMIP5 and CMIP6 Models

Thomas Oudar, Julien Cattiaux, Hervé Douville

AGU100 ADVANCING EARTH AND SPACE SCIENCE

Geophysical Research Letters

RESEARCH LETTER
10.1029/2019GL086695

Drivers of the Northern Extratropical Eddy-Driven Jet Change in CMIP5 and CMIP6 Models

Thomas Oudar[1], **Julien Cattiaux**[1], **and Hervé Douville**[1]

[1]CNRM, Université de Toulouse, Météo France, CNRS, Toulouse, France

Key Points:
- Ensemble mean biases and projections of 850 hPa zonal wind are consistent between CMIP5 and CMIP6 models
- Intermodel spread remains high but can be related to a limited number of remote tropical and extratropical drivers
- Model biases in the jet stream position also contribute significantly to the spread

Supporting Information:
- Supporting Information S1

Correspondence to:
T. Oudar,
thomas.oudar@meteo.fr

Citation:
Oudar, T., Cattiaux, J., & Douville, H. (2020). Drivers of the northern extratropical eddy-driven jet change in CMIP5 and CMIP6 models. *Geophysical Research Letters*, *47*, e2019GL086695. https://doi.org/10.1029/2019GL086695

Received 19 DEC 2019
Accepted 15 MAR 2020
Accepted article online 18 MAR 2020

Abstract The wintertime midlatitude atmospheric circulation is evaluated in CMIP6 models. The biases have been reduced since CMIP5 although the low-level flow is still too zonal. CMIP5 and CMIP6 projections of 850 hPa zonal wind are then analyzed and are consistent under the RCP8.5 and the SSP5–8.5 scenarios, respectively. A poleward shift is identified in the Pacific, while a tripole structure is found in the North Atlantic: The zonal wind strengthens over Western Europe and decreases north and south. A multiple linear regression allows us to quantify the contribution of different drivers to the intermodel spread in zonal wind projections. It supports the importance of projected tropical warming and changes in the stratospheric vortex but also suggests a contribution of the asymmetry in the projected surface warming of the equatorial Pacific and of the present-day biases in the eddy-driven jet position. The North Atlantic warming hole plays a weaker role.

Plain Language Summary The projection of the midlatitude atmospheric circulation is highly uncertain. Climate models exhibit a significant ensemble dispersion although some robust signals seem to emerge at the end of the 21st century: a poleward shift of the 850 hPa zonal wind in the Pacific and a strengthening over Northern Europe. This response is consistent between the former and current-generation global climate models. Several drivers have been proposed to explain this response. Here, it is confirmed that the amplified warming of the tropical high troposphere and variation of the stratospheric vortex play a more important role than the amplified warming over the Arctic. In addition, it is suggested that the West-East temperature gradient in the tropical Pacific and the biases of the jet position have a significant contribution, as opposed to the minimum warming in the North Atlantic.

1. Introduction

Projections of the wintertime Northern Hemisphere eddy-driven jet are highly uncertain (Gao et al., 2016; Woollings, 2010). CMIP5 multimodel mean projections exhibit a poleward shift of the zonal wind in the Pacific and a tripole structure in the Atlantic characterized by increased storminess over Western Europe (Pachauri et al., 2014; Peings et al., 2018; Ulbrich et al., 2008), yet with a substantial intermodel spread. Understanding such model discrepancies is crucial in order to better constrain climate projections of midlatitude weather characteristics. Uncertainties can be explained by several factors including the opposite influence of Arctic amplification and upper-tropospheric tropical warming (McCusker et al., 2017; Oudar et al., 2017; Screen et al., 2018). Several studies have indeed found that the upper-troposphere tropical warming is associated with a poleward shift of the zonal wind (Barnes & Polvani, 2013; Harvey et al., 2014; Yin, 2005) while the surface Arctic amplification could cause an equatorward shift (Barnes & Polvani, 2015; Screen et al., 2018). Other potential drivers include the response of the stratospheric vortex (Manzini et al., 2018; Zappa & Shepherd, 2017); in particular, Zappa and Shepherd (2017) (hereinafter ZS17) have suggested that it may have a greater effect on the midlatitude zonal wind response than the Arctic amplification. It has also been shown that the North Atlantic warming hole (i.e., the minimum warming observed in the subpolar gyre) could significantly modify the baroclinicity, hence the zonal wind, over the Euro-Atlantic region (Gervais et al., 2019). Future changes in the tropical Pacific can also affect the midlatitude circulation through teleconnections and Rossby wave propagation (Brönnimann, 2007; Ciasto et al., 2016; Toniazzo & Scaife, 2006). Finally, most coupled models tend to have the eddy-driven jet position too equatorward compared to the observed position (see Figures S1 and S2), a systematic bias which is likely to explain the spread of the projected circulation response to climate change (Gao et al., 2016).

In order to quantify individual contributions of these potential factors to the intermodel dispersion in the midlatitude circulation response, ZS17 have proposed a multiple linear regression framework. They have fitted a regression model between the zonal wind response and three potential drivers: the Arctic amplification (AA), the tropical amplification (TA), and the polar vortex strength (PVS). They found that the AA has a relatively weak impact while a strong vortex induces a poleward shift of the eddy-driven jet and a strong warming in the tropical high troposphere is associated with the tripolar structure over the North Atlantic mentioned in the previous paragraph. It is of main interest to test whether these results are reproducible when using the new generation climate models, that is, whether the fit of the linear regression model is robust across CMIP5 and CMIP6 ensembles. It is also interesting to assess the role of the other potential drivers mentioned above in such a multiple regression framework.

In this paper, we evaluate the representation of the Northern Hemisphere eddy-driven jet in the new generation of coupled models from the sixth phase Coupled Model Intercomparison Project (CMIP6). We document the future changes in the CMIP6 climate projections at the end of the 21st century which we compare with the previous generation models (CMIP5). Projected changes are illustrated with the wintertime 850 hPa zonal wind and a diagnostic characterizing the latitudinal position of the eddy-driven jet in various sectors. Model response uncertainties are interpreted as the result of several drivers, and the mechanisms are briefly discussed. Our questions can be summarized as follows:

1. Has the wintertime Northern Hemisphere midlatitude atmospheric circulation been improved between CMIP5 and CMIP6 models?
2. What are the future projections in CMIP6? Are they comparable to CMIP5 projections?
3. What are the main drivers at play?

Section 2 describes the model outputs used in this study, the different metrics and diagnostics, and the multiple linear regression analysis. Results are presented in section 3. Finally, we discuss the results and conclude in section 4.

2. Methods

2.1. CMIP5 and CMIP6 Models

In this study we use monthly outputs from 29 CMIP5 and 22 CMIP6 models (listed in supporting information Tables S1 and S2). One ensemble member for each model has been used, and all models have been interpolated on a common grid (T127). The projected wind anomalies are calculated as the difference between the end of the 21st century (2080–2099) and the pre-industrial period (1861–1900), and we focus on an extended winter season from October to March (ONDJFM). For the projections, the parallel RCP8.5 and the SSP5–8.5 are used for CMIP5 and CMIP6, respectively. Even if the CO_2 and CH_4 emissions are respectively higher and lower in the SSP5–8.5 compared to the RCP8.5 (Gidden et al., 2019), the evolution of global mean temperature is comparable between the two scenarios (not shown). We thus consider that the two families of scenarios are relatively close to each other (O'Neill et al., 2016) and that mixing them in the present study is not an issue. Assessing projected changes from differences between the pre-industrial period and the highest concentration pathway allows to maximize the signal, hence the model dispersion. We also use the ERA5 reanalysis for the model evaluation (C3S, 2017).

2.2. Metrics

We first use a set of three metrics defined following Peings et al. (2018). These metrics are similar to the metrics used by ZS17, albeit with slightly different definitions (e.g., selected levels and longitude-latitude boxes):

- Arctic amplification (AA): temperature change averaged between 1,000–700 hPa and 60–90°N;
- tropical amplification (TA): temperature change averaged between 400–150 hPa and 20°S to 20°N; and
- polar vortex strength (PVS): zonal mean zonal wind change averaged between 250–30 hPa and 70–90°N.

In addition, we define three other metrics that characterize other potential drivers of changes in the midlatitude dynamics and/or the North Atlantic jet stream:

- surface temperature difference between the NINO4 region (5°S to 5°N/160°E to 150°W) and the NINO3 region (5°S to 5°N/150–90°W). This driver is noted "NINO4-NINO3";
- surface temperature in the North Atlantic warming hole region (35–60°N/40–10°W, NAWH); and

Table 1
Correlation Between Each Drivers' Responses Before (Top) and After (Bottom) Scaling by Global Warming

	AA	TA	PVS	NINO	NAWH	Jet bias
AA	1					
TA	**0.7**	1				
PVS	−0.1	0	1			
NINO	−0.1	0.2	0	1		
NAWH	**0.8**	**0.5**	0	−0.2	1	
Jet bias	0.2	0.1	−0.2	−0.1	0.2	1
AA	1					
TA	−0.1	1				
PVS	−0.1	0	1			
NINO	**−0.3**	**0.3**	0	1		
NAWH	**0.4**	**−0.3**	−0.1	−0.2	1	
Jet bias	0	**−0.3**	−0.2	0	0.1	1

Note. Bold font indicates significant correlation at the 95% confidence level. Significance is assessed through the calculation of $t = r * \frac{N-2}{1-r^2}$, with r the correlation coefficient and N the number of models, which follow a Student t distribution.

- jet position bias against ERA5 in the Central Atlantic region. Note that the bias is estimated by subtracting the ONDJFM mean eddy-driven jet position over the period 1979–2018 in ERA5 to each model mean eddy-driven jet position over the same period.

The position of the eddy-driven jet is defined as in Woollings et al. (2010) and Oudar et al. (2020). Here, we use monthly outputs in order to increase the number of available models. In Oudar et al. (2020), we have checked that using monthly outputs instead of daily outputs in the calculation of the eddy-driven jet position does not affect the result. First, the zonal wind is averaged over the levels 850 and 700 hPa and then zonally averaged over the region of interest (North Pacific, Central Atlantic, and Western Europe). The maximum wind position is identified as the latitude at which the wind speed is maximum. Finally, a parabola is fitted on the zonal wind speed taken over a 11-gridpoint window centered on the first guess, and the maximum wind position corresponds to the maximum of the parabola. It is defined over three different regions: the North Pacific (20–90°N/120–240°E), the North Atlantic (20–90°N/60°W to 0) and western Europe (20–90°N/0–30°E).

2.3. Multiple Linear Regression

We follow the method applied in ZS17, but with the CMIP5 and CMIP6 models mixed together. The wintertime 850 hPa zonal wind response can be expressed as a function of the different drivers defined in section 2.2. For a location x and a model m:

$$\begin{aligned}\Delta U850_{xm} = a_x + b_x(\Delta T_{AA})_m + c_x(\Delta T_{TA})_m + d_x(\Delta U_{PVS})_m \\ + e_x(\Delta T_{NAWH})_m + f_x(\Delta T_{NINO4-NINO3})_m + g_x(Bias)_m \\ + h_{xm},\end{aligned} \tag{1}$$

where b_x, c_x, d_x, e_x, f_x, and g_x correspond to the regression coefficients associated with each driver, a_x is the intercept, and h_{xm} is the residual term. Note that the multiple linear regression does not imply the causality between the so-called drivers and the projected response of the low-level zonal wind. Yet this framework allows us to diagnose the percentage of intermodel spread in the wind response which is associated with those large-scale climate indices.

As in ZS17, all drivers are scaled by the global near-surface warming in each model and standardized relative to the multimodel mean and standard deviation. This scaling strongly reduces the potential dependencies between the predictors used in the regression (equation (1)), as illustrated by the cross correlations shown in Table 1. For instance, the significantly positive correlation between the AA and TA is lost after scaling, suggesting that models with the highest AA and TA also have the highest global warming. A few significant

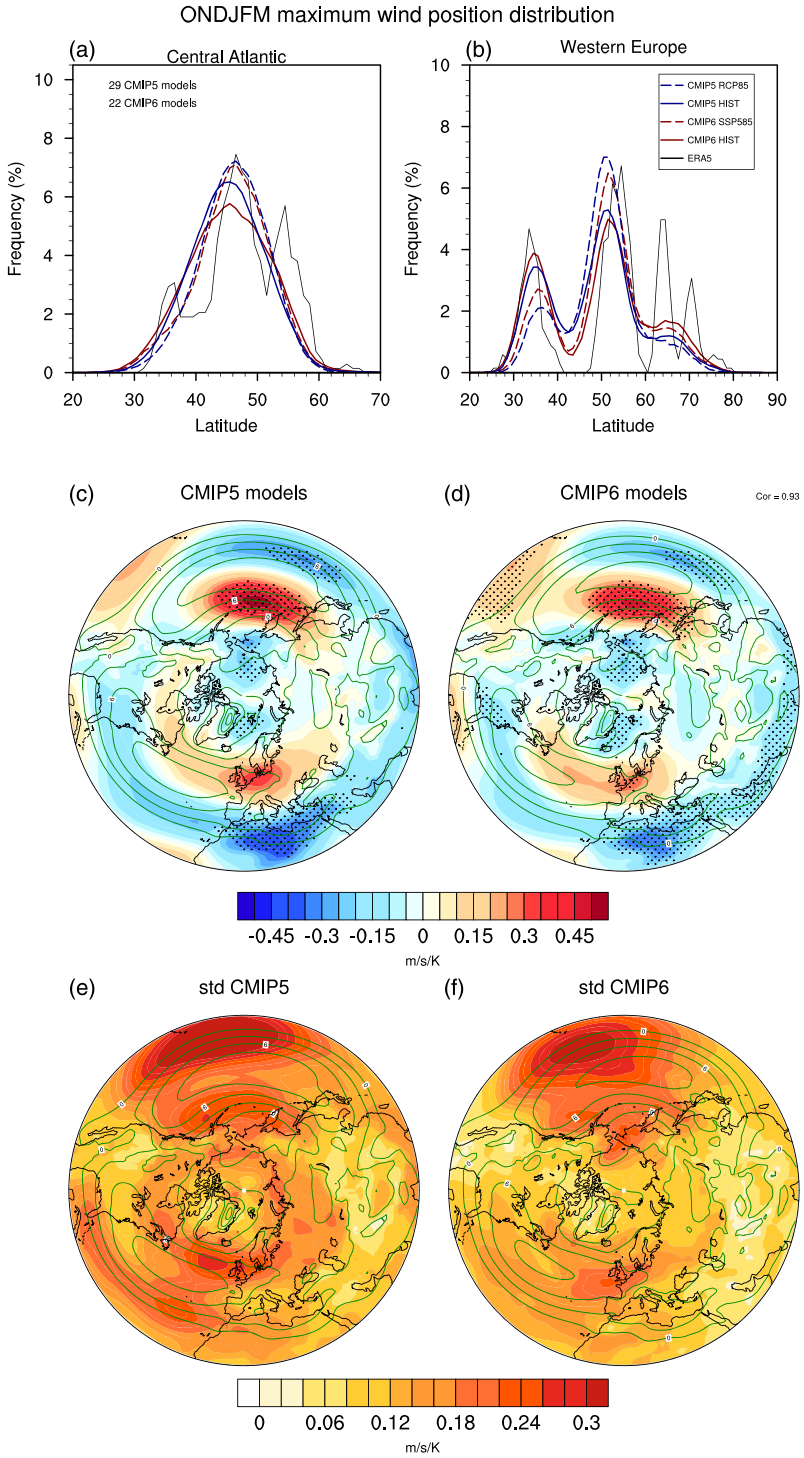

Figure 1. (a, b) Probability distribution function of the maximum wind position in ERA5 (black line), the CMIP5 (CMIP6) historical ensemble mean averaged over the period 1861–1900 in solid blue line (solid red line), the CMIP5 RCP85 (CMIP6 SSP5–8.5) ensemble mean averaged over the period 2080–2099 in dashed blue line (dashed red line) for the Central Atlantic region (20–90°N/60°W to 0) and the western Europe region (20–90°N/0–30°E), respectively; (c, d) 850 hPa zonal wind response, scaled by global warming, between the end of the 21st century (2080–2099) and the pre-industrial period (1861–1900) for the CMIP5 and CMIP6 ensemble mean, respectively. Stippling indicate significance at the 95% confidence level according to a *t* test, computed following Wilks (2006). The correlation between the two patterns is shown on the top right corner of panel (d). (e, f) Standard deviation across CMIP5 and CMIP6 models, respectively. Green contours in panels (c–f) correspond to the 850 hPa zonal wind climatological mean of the historical simulations (contours from 0 to 12 by 3 m/s).

correlations remain after scaling, for example, between AA and NAWH in agreement with the possible role of ocean heat advection on both North Atlantic SST and Arctic sea-ice extent. However, these correlations remain small and do not exclude additive effects of the different drivers on the zonal wind response.

3. Results

3.1. Consistency Between CMIP5 and CMIP6 Projections

We first evaluate the representation of the midlatitude atmospheric circulation in CMIP5 and CMIP6 models. The 850 hPa zonal wind bias has been reduced between CMIP5 and CMIP6, although the midlatitude flow is still too zonal as compared to ERA5 reanalysis (see Figures S1 and S2 which shows the 850 hPa zonal wind biases for each model and the ensemble mean). Besides, the tripole structure in the low-troposhere eddy-driven jet position observed in ERA5 over the Central Atlantic (Figure 1a) is not captured by either CMIP5 or CMIP6 historical ensemble mean. Over Western Europe (Figure 1b), CMIP5 and CMIP6 ensemble mean are relatively close to the ERA5 distribution, except in the northern latitudes (above 60°N). Both CMIP6 and CMIP5 projections (dashed red and blue lines) show a slight squeezing of the eddy-driven jet position, more pronounced over Western Europe, in good agreement with the results of Peings et al. (2018) based on CMIP5 models. This squeezing is also well identified over Western Europe when looking at maps of the 850 hPa zonal wind projections in CMIP5 (Figure 1c) and CMIP6 (Figure 1d). Note that responses shown in panels (c) and (d) have been scaled by global warming. In the North Pacific, the 850 hPa zonal wind significantly shifts poleward in both CMIP5 and CMIP6 projections which are very consistent. The spatial anomaly pattern correlation is of about 0.94, and the midlatitude changes are robust between the two ensembles. We thus decide to mix CMIP5 and CMIP6 models in the analysis presented in the rest of the paper. However, we are aware that the statistical independence of models is not always a valid assumption (Knutti et al., 2013) and that caution is needed in multimodel analysis. We have verified that our results remain similar (although less statistically significant) when performing the regression analysis on subsets of CMIP5 and CMIP6 models separately (see Figure S3 for the case with only CMIP6 models), and when selecting only one model per modeling center (not shown). Lastly, panels (e) and (f) in Figure 1 show the standard deviation of the response for CMIP5 and CMIP6 ensembles, respectively. Maximum are localized in the Central Atlantic, Northern Europe, and in the Pacific south of the maximum 850 hPa zonal wind climatology. The spread is reduced in CMIP6 compared to CMIP5, but it is still significant. In the following we thus investigate the source of the uncertainties in this response.

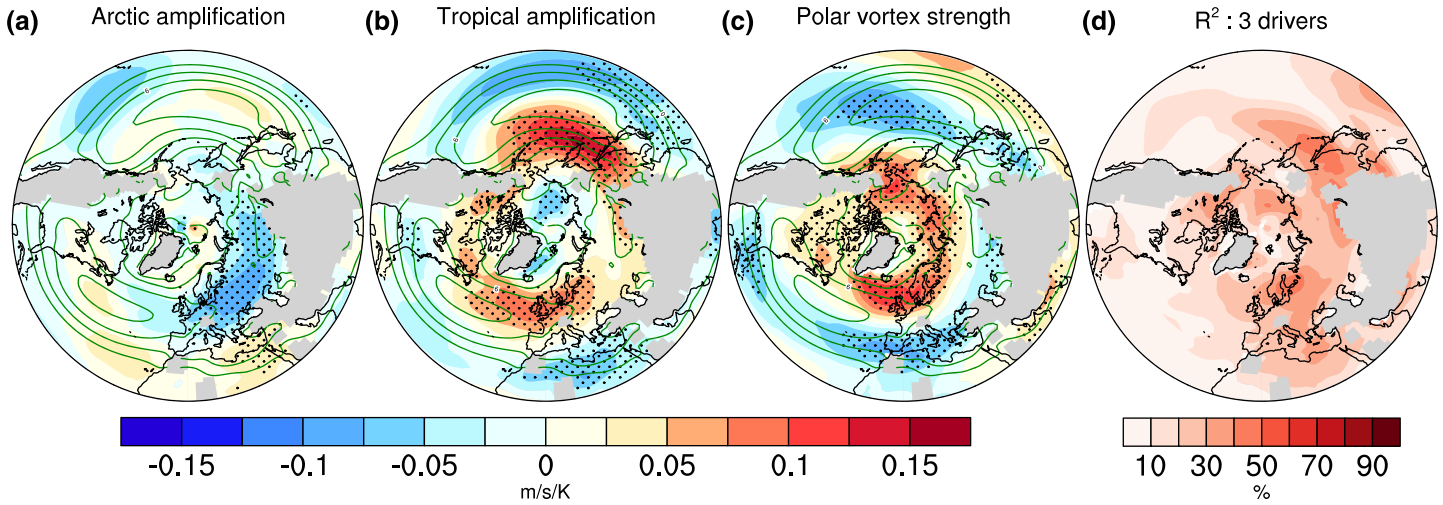

Figure 2. Multiple linear regression between the 850 hPa zonal wind response in CMIP5 and CMIP6 models and the three remote drivers used in Zappa and Shepherd (2017) for ONDJFM; (a) 850 hPa zonal wind response scaled by global warming (m/s/K) associated with one sigma positive anomaly in the polar amplification in the CMIP5 + CMIP6 intermodel spread. Green contours correspond to the climatological mean estimated as the multimodel mean of the historical simulations. Stippling indicate regression coefficients that are significant at the 95% confidence level. (b, c) Same as (a) but for the tropical amplification and the polar vortex strength, respectively. The fraction of variance explained by these three predictors is shown on panel (d) (in %).

3.2. Expanding ZS17 Regression to CMIP6 Models

Following ZS17, we first apply a point-wise multiple linear regression between CMIP5 + CMIP6 zonal wind projections and three drivers: the Arctic amplification, the tropical amplification, and the polar vortex strength. Thus, the patterns shown in Figure 1 can be expressed as a function of the three drivers (in a similar way as in equation (1)).

Figure 2 shows the regression coefficient for each of the three drivers. Overall, this figure agrees well with Figure 3 of ZS17 who only used CMIP5 models. In particular, we confirm that the effect of the Arctic amplification is rather weak, although a high AA is characterized by weaker zonal winds over Europe and Siberia. We find a weaker signal in the North Pacific associated to AA compared to ZS17. The effect of the tropical amplification is stronger and characterized by a poleward shift of the zonal wind in the North Pacific, and a tripole structure in the North Atlantic: The zonal wind increases over Northern Europe and decreases over North Africa and the Greenland sea. This pattern is in line with previous studies (e.g., Peings et al., 2018). Finally, the effect of the polar vortex strength results in a dipole pattern with positive anomalies northward and negative anomalies southward in both Atlantic and Pacific regions. This is also in agreement with ZS17 although they found a stronger signal in the Atlantic than in the Pacific. The fraction of variance explained by these three drivers (i.e., the R^2 coefficient) is shown in Figure 2d. It is maximum over Western and Northern Europe and Western Pacific. Again, it is in agreement with the Figure 4 of ZS17.

We therefore consider that the regression analysis presented in ZS17 remains valid when aggregating the CMIP6 models to the CMIP5 ensemble, even with slightly different definitions of the predictors. Also note that—contrarily to ZS17—we have kept all models in the analysis, even models that could have been considered as outliers given their limited performance in present-day climate.

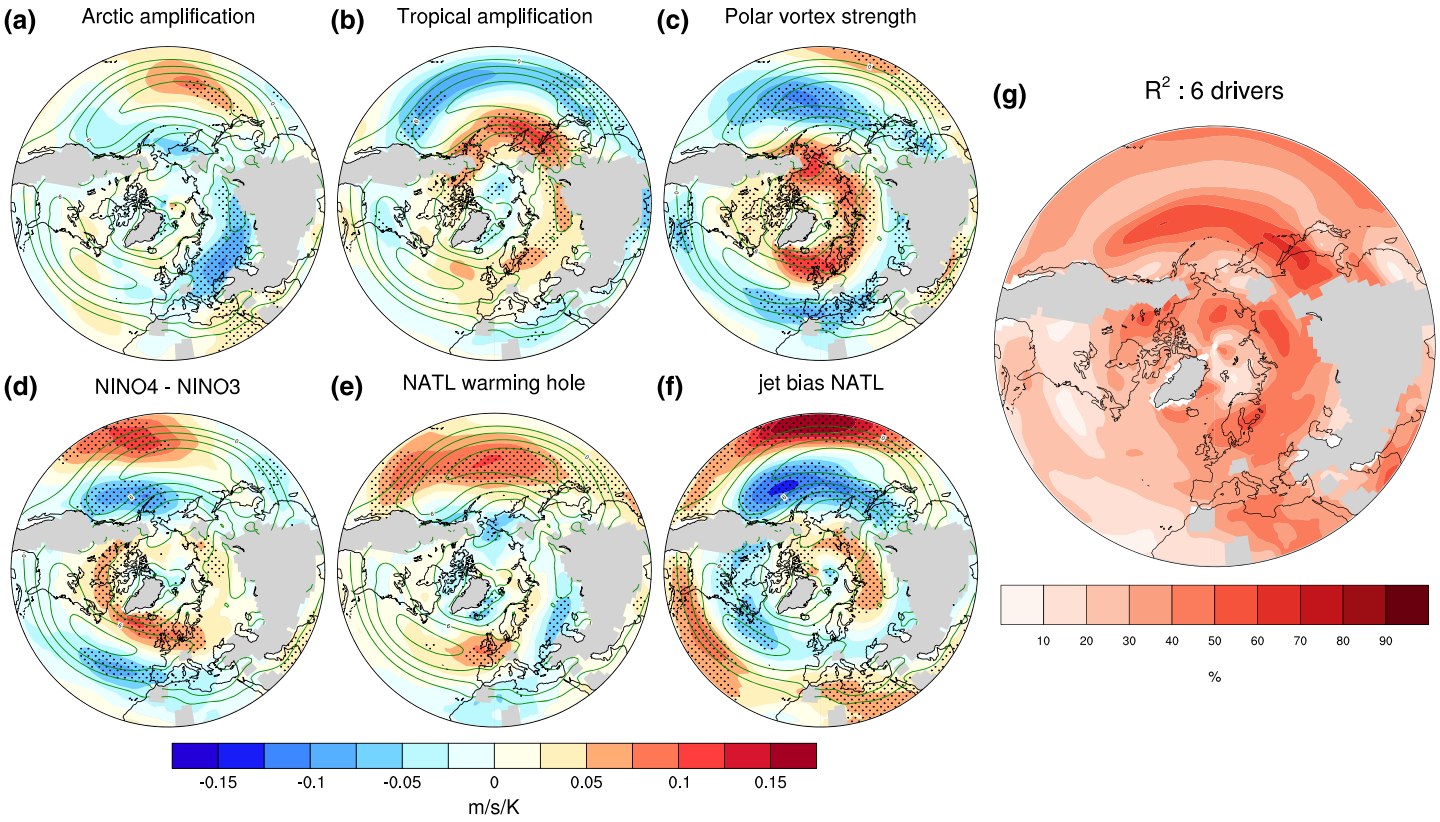

Figure 3. Same as Figure 4 but with more predictors added to the regression: (a) polar amplification, (b) tropical amplification, (c) polar vortex strength, (d) surface temperature difference between the NINO4 box and the NINO3 box, (e) surface temperature in the North Atlantic warming hole, and (f) the jet position bias in the North Atlantic against ERA5. The fraction of variance explained by these six predictors is shown on panel (g) (in %).

3.3. Additional Potential Drivers

Adding CMIP6 models to the regression analysis supports the main results found by ZS17. Thus, we now take advantage of the increased number of models to add new potential predictors that can further explain the intermodel spread. Here we propose to investigate the role of three scaled drivers: the West-East surface temperature gradient in the tropical Pacific, the averaged surface temperature in the North Atlantic warming hole region (note that this driver is multiplied by −1 so that the regression coefficient found is associated with a deep warming hole), and the eddy-driven jet position bias over the North Atlantic.

Figure 3 shows the regressions coefficients for the six drivers and the fraction of variance explained associated with these six drivers (panel g). When adding the three other predictors, the regression coefficients associated with the first three drivers are not significantly changed, suggesting the relative independence of all six drivers (Figures 2a–2c and 3a–3c). However, some changes are identified, especially over the Atlantic sector. An important change is the absence of tripole pattern in response to TA. This tripole pattern seems to be a combination between the latter, the temperature gradient in the tropical Pacific, and the NAWH. A pronounced NAWH has an influence in the Atlantic but also in the Pacific: The zonal wind strengthens over Western Europe and most of the Pacific (Figure 3e). In the Atlantic, a possible mechanism is that the warming hole causes a local increase of the meridional temperature gradient and thus an increase of the zonal wind. This result is in line with Gervais et al. (2019) who investigated the North Atlantic jet response to the Warming hole in the CESM climate model.

A strengthened West-East temperature gradient in the tropical Pacific is associated with a poleward shift of the zonal wind in the Atlantic and a southward shift in the Eastern Pacific (Figure 3d). The pattern in the Pacific resembles the one found in Cattiaux and Cassou (2013) who investigated the CMIP3/CMIP5 differences in the Northern Annular Mode (NAM) projections. They found that a stronger relative warming of the western tropical Pacific in CMIP5 than in CMIP3 is associated with a negative NAM response due to a Rossby wave train. Similarly, Ciasto et al. (2016) found that the eastward extension of the North Atlantic storm tracks could be related to the SST in the western Pacific that trigger a Rossby wave. Figures 3d and 3e suggest that the squeezing of the variability over Western Europe could be a result of both the North Atlantic warming hole and the asymmetry in the tropical Pacific warming (Ciasto et al., 2016). This result suggests that the northern midlatitude circulation response can show zonal asymmetries due to the interplay between the multiple potential drivers of the North Atlantic eddy-driven jet.

The position of the eddy-driven jet in the Atlantic also exhibits significant responses: It corresponds to a dipole with negative anomalies northward the maximum climatology and positive anomalies southward

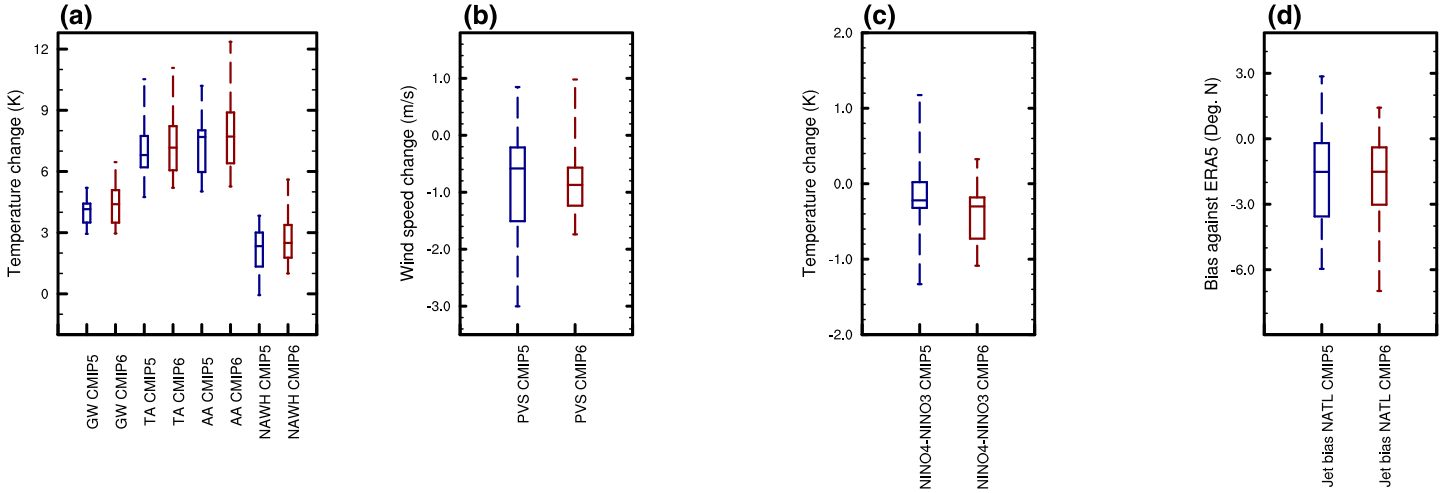

Figure 4. Response of the remote drivers defined in section 2 (2080–2099 minus 1861–1900), in red for CMIP6 models and in blue for CMIP5 models: (a) global near-surface warming (GW), tropical amplification (TA), Arctic amplification (AA), and surface temperature in the North Atlantic warming hole (NAWH); (b) Polar Vortex Strength (PVS); and (c) West-East temperature gradient in the tropical Pacific (NINO4-NINO3). The present-day bias in the North-Atlantic jet position is also indicated in panel (d). Boxplots show the multimodel median (central segment), the first and third quartile range (box), and the minimum and maximum (whiskers).

(Figure 3f). It means that models that have a stronger negative bias in the present-day eddy-driven jet position tend to project a more pronounced poleward shift in a warmer world and are more sensitive to the tropical amplification. In other words, if a model has a positive bias it can be less sensitive since it is less likely to project on a potential poleward shift.

Figure 3g shows the fraction of variance explained by these six drivers. Adding the three new drivers increases the R^2 almost everywhere, especially over eastern Pacific and western Atlantic. It is not surprising since the R^2 necessarily increases when adding predictors to a linear regression model, but the fact that it reaches 0.6 to 0.7 in some regions nevertheless suggests that the new predictors are informative. The use of more sophisticated statistical tools to select the best combination of predictors is considered to be beyond the scope of this study and will need further investigations. However, the individual impact of the three additional drivers is shown in Figure S4. The NAWH has little impact on the R^2, except in the Pacific, surprisingly (see Figure S4a). More investigations will be undertaken in the future to understand the response to the warming hole. The bias in the eddy-driven jet position in the North Atlantic is associated with increased explained variance over the subtropical regions at a latitude band around 45°N (Figure S4b). The temperature gradient in the tropical Pacific increases the explained variance at around 60°N in the Atlantic and North America, over Southern Europe and eastern Pacific (Figure S4c).

4. Discussion and Conclusion

We haveinvestigated the wintertime 850 hPa zonal wind and eddy-driven jet position in historical simulations and low-mitigation scenarios with both CMIP5 and CMIP6 models. The present-day zonal wind biases have been reduced between CMIP5 and CMIP6, even if the CMIP6 multimodel ensemble mean is still characterized by a too zonal flow. The two ensembles exhibit very similar responses at the end of the 21st century: The zonal wind shifts poleward in the Pacific while it is squeezed and strengthened over Northern Europe, yet with a substantial intermodel spread. These results suggest that no major change has occurred from one model generation to the next and that a more accurate and quantitative assessment is still hampered by large model uncertainties, including over continental regions such as Western Europe for example.

To explain the intermodel spread in climate projections, several drivers have been proposed in the literature: the Arctic amplification, the upper-troposphere tropical amplification, and the stratospheric vortex. In addition, we have also tested the role of the West-East surface temperature gradient in the tropical Pacific, the average surface temperature in the North Atlantic warming hole region, and the bias in the eddy-driven jet position in the North Atlantic. By design, adding more predictors helps to increase the explained variance and the effective added value of the additional predictors will need further investigation. The tropical surface temperature gradient and the position bias significantly increase the variance explained in some regions, whereas the North Atlantic warming hole plays a weaker role. Our analysis suggests the importance to add more predictors in the linear regression model.

Once the main contributors to the intermodel spread in the midlatitude circulation have been identified, a legitimate question is whether the uncertainty in the response of each individual driver can be reduced. As shown in Figure 4, the projections of the different drivers exhibit a significant spread across both CMIP5 and CMIPmodels. The two ensembles exhibit a comparable warming ranged between 5 and 12 °C over the Arctic and in the tropical high troposphere (Figure 4a). CMIP6 models still show a minimum warming over the North Atlantic warming hole region, although it is less pronounced than in CMIP5 models. The stratospheric vortex weakens in most models and the uncertainty is slightly reduced in CMIP6 compared to CMIP5 (Figure 4b). The spread of the West-East temperature gradient is reduced in CMIP6 compared to CMIP5, because of a stronger warming over the NINO3 region in CMIP6 (Figure 4c). Most models in CMIP5 and CMIP6 tend to have a negative bias of the eddy-driven jet position in the Central Atlantic region (Figure 4d, see also Figures S1 and S2). Overall, we find that the uncertainties associated with the response of each individual driver have not been significantly reduced between CMIP5 and CMIP6. Future work may involve searching for observational constraints (Hall et al., 2019), that is, testing whether future responses of the remote drivers may be correlated to their present-day behaviors. Using an as-large-as-possible multimodel ensemble is helpful to build such statistical relationships, and this study shows that CMIP5 and CMIP6 models can be mixed for this purpose.

Acknowledgments
We would like to thank one anonymous reviewer for his helpful comments to improve the manuscript. This study was funded by the European Union's Horizon 2020 Research and Innovation program under Grant Agreement 727862. We acknowledge the World Climate Research Programme, which, through its Working Group on Coupled Modelling, coordinated and promoted CMIP6. We thank the climate modeling groups for producing and making available their model output, the Earth System Grid Federation (ESGF) for archiving the data and providing access, and the multiple funding agencies who support CMIP6 and ESGF. CMIP6 and CMIP5 outputs are available online (https://esgf-node.ipsl.upmc.fr/projects/esgf-ipsl/). The authors thank Aurélien Ribes for discussion of the results.

References

Barnes, E. A., & Polvani, L. (2013). Response of the midlatitude jets, and of their variability, to increased greenhouse gases in the CMIP5 models. *Journal of Climate*, *26*(18), 7117–7135.
Barnes, E. A., & Polvani, L. M. (2015). CMIP5 projections of Arctic amplification, of the north american/North Atlantic circulation, and of their relationship. *Journal of Climate*, *28*(13), 5254–5271.
Brönnimann, S. (2007). Impact of El Niño–Southern Oscillation on European climate. *Reviews of Geophysics*, *45*, RG3003. https://doi.org/10.1029/2006RG000199
Cattiaux, J., & Cassou, C. (2013). Opposite CMIP3/CMIP5 trends in the wintertime northern annular mode explained by combined local sea ice and remote tropical influences. *Geophysical Research Letters*, *40*, 3682–3687. https://doi.org/10.1002/grl.50643
Ciasto, L. M., Li, C., Wettstein, J. J., & Kvamstø, N. G. (2016). North Atlantic storm-track sensitivity to projected sea surface temperature: Local versus remote influences. *Journal of Climate*, *29*(19), 6973–6991.
Copernicus Climate Change Service (C3S). (2017). Era5: Fifth generation of ECMWF atmospheric reanalyses of the global climate.
Gao, Y., Lu, J., & Leung, L. R. (2016). Uncertainties in projecting future changes in atmospheric rivers and their impacts on heavy precipitation over Europe. *Journal of Climate*, *29*(18), 6711–6726.
Gervais, M., Shaman, J., & Kushnir, Y. (2019). Impacts of the North Atlantic warming hole in future climate projections: Mean atmospheric circulation and the North Atlantic jet. *Journal of Climate*, *32*(10), 2673–2689.
Gidden, M., Riahi, K., Smith, S., Fujimori, S., Luderer, G., Kriegler, E., et al. (2019). Global emissions pathways under different socioeconomic scenarios for use in CMIP6: A dataset of harmonized emissions trajectories through the end of the century. *Geoscientific Model Development Discussions*, *12*(4), 1443–1475.
Hall, A., Cox, P., Huntingford, C., & Klein, S. (2019). Progressing emergent constraints on future climate change. *Nature Climate Change*, *9*(4), 269–278.
Harvey, B., Shaffrey, L., & Woollings, T. (2014). Equator-to-pole temperature differences and the extra-tropical storm track responses of the CMIP5 climate models. *Climate dynamics*, *43*(5-6), 1171–1182.
Knutti, R., Masson, D., & Gettelman, A. (2013). Climate model genealogy: Generation CMIP5 and how we got there. *Geophysical Research Letters*, *40*, 1194–1199. https://doi.org/10.1002/GRL.50256
Manzini, E., Karpechko, A. Y., & Kornblueh, L. (2018). Nonlinear response of the stratosphere and the North Atlantic-European climate to global warming. *Geophysical Research Letters*, *45*, 4255–4263. https://doi.org/10.1029/2018GL077826
McCusker, K. E., Kushner, P. J., Fyfe, J. C., Sigmond, M., Kharin, V. V., & Bitz, C. M. (2017). Remarkable separability of circulation response to Arctic sea ice loss and greenhouse gas forcing. *Geophysical Research Letters*, *44*, 7955–7964. https://doi.org/10.1002/2017GL074327
O'Neill, B. C., Tebaldi, C., van Vuuren, D. P., Eyring, V., Friedlingstein, P., Hurtt, G., et al. (2016). The scenario model intercomparison project (scenariomip) for CMIP6. *Geoscientific Model Development*, *9*(9), 3461–3482.
Oudar, T., Cattiaux, J., Douville, H., Geoffroy, O., Saint-Martin, D., & Roehrig, R. (2020). Robustness and drivers of the northern hemisphere extratropical atmospheric circulation response to a CO_2-induced warming in CNRM-CM6-1. *Climate Dynamics*, *54*, 2267–2285.
Oudar, T., Sanchez-Gomez, E., Chauvin, F., Cattiaux, J., Terray, L., & Cassou, C. (2017). Respective roles of direct GHG radiative forcing and induced Arctic sea ice loss on the northern hemisphere atmospheric circulation. *Climate Dynamics*, *49*(11–12), 3693–3713.
Pachauri, R. K., Allen, M. R., Barros, V. R., Broome, J., Cramer, W., Christ, R., et al. (2014). Climate change 2014: Synthesis report. In R. Pachauriand & L. Meyer et al. (Eds *Contribution of working groups I, II and III to the fifth assessment report of the intergovernmental panel on climate change* (pp. 151). Geneva, Switzerland: IPCC, ISBN: 978-92-9169-143-2.
Peings, Y., Cattiaux, J., Vavrus, S. J., & Magnusdottir, G. (2018). Projected squeezing of the wintertime North-Atlantic jet. *Environmental Research Letters*, *13*(7), 74,016.
Screen, J. A., Deser, C., Smith, D. M., Zhang, X., Blackport, R., Kushner, P. J., et al. (2018). Consistency and discrepancy in the atmospheric response to Arctic sea-ice loss across climate models. *Nature Geoscience*, *11*(3), 155.
Toniazzo, T., & Scaife, A. A. (2006). The influence of ENSO on winter North Atlantic climate. *Geophysical Research Letters*, *33*, L24704. https://doi.org/10.1029/2006GL027881
Ulbrich, U., Pinto, J. G., Kupfer, H., Leckebusch, G., Spangehl, T., & Reyers, M. (2008). Changing northern hemisphere storm tracks in an ensemble of IPCC climate change simulations. *Journal of Climate*, *21*(8), 1669–1679.
Wilks, D. (2006). On "field significance" and the false discovery rate. *Journal of Applied Meteorology and Climatology*, *45*(9), 1181–1189.
Woollings, T. (2010). Dynamical influences on European climate: An uncertain future. *Philosophical Transactions of the Royal Society A: Mathematical, Physical and Engineering Sciences*, *368*(1924), 3733–3756.
Woollings, T., Hannachi, A., & Hoskins, B. (2010). Variability of the North Atlantic eddy-driven jet stream. *Quarterly Journal of the Royal Meteorological Society*, *136*(649), 856–868.
Yin, J. H. (2005). A consistent poleward shift of the storm tracks in simulations of 21st century climate. *Geophysical Research Letters*, *32*, L18701. https://doi.org/10.1029/2005GL023684
Zappa, G., & Shepherd, T. G. (2017). Storylines of atmospheric circulation change for European regional climate impact assessment. *Journal of Climate*, *30*(16), 6561–6577.